Structure Organization of Silicate Polyanions with Surfactants: A New Approach to the Syntheses, Structure Transformations, and Formation Mechanisms of Mesostructural Materials

Colin A. Fyfe* and Guoyi Fu

Contribution from the Department of Chemistry, University of British Columbia, 2036 Main Mall, Vancouver, B.C. V6T 1Z1, Canada

Received October 10, 1994. Revised Manuscript Received June 12, 1995[⊗]

Abstract: Structure organization of the cubic silicate species, $Si_8O_{20}^{8-}$ (Si_8), by the cationic surfactant, $CH_3(CH_2)_{15}N(CH_3)_3^+$, leads to mesophasic precipitates with layer or rod-based structures depending on the conditions of the precipitation. Further ordering of the structures of these precipitates has been achieved by acidic vapor treatment leading to ordered materials with cubic (MCM-48), lamellar, and hexagonal (MCM-41) mesostructures. For the first time, step-by-step structural transformations have been observed, which follow the sequence given here, during vapor phase treatment: layered precipitate (L_0) → cubic (V_1) → lamellar (L_1) → hexagonal (H_1). These results strongly support a mechanism in which, under typical synthetic conditions, silicates and surfactants mutually organize into mesoscopic assemblies with geometries close to those of discs, rods, or spheres as determined by charge density matching and then these assemblies further condense into ordered lamellar, hexagonal, or cubic structures depending on the final reaction conditions. The present results also demonstrate that it is possible to achieve structure-tailoring and better framework ordering of these mesostructural materials.

Introduction

Since the researchers at Mobil Corp. recently published their pioneering work on silicate− and aluminosilicate−surfactant mesostructural materials, designated M41'S,[1,2] considerable research efforts have been made in this area in the investigation of the synthesis,[3,4] formation mechanism,[5−7] structure,[8,9] and other aspects[10−19] of the reaction. Potential applications of these materials as either highly ordered mesoporous solids or as organic−inorganic nanocomposites have been discussed including applications in the area of biomimetics.[20] So far, four different mesostructures have been reported, namely, a hexagonal phase (MCM-41), two types of cubic phase with space groups *Ia3d* (MCM-48) and *Pm3n*, respectively, and a lamellar phase. Figure 1 schematically shows the structure of three of these phases. Metal oxides other than silica and alumina, such as titanium oxide[21−24] and vanadium oxide,[25] have also been incorporated into the hexagonal structures. Different mechanisms for the formation of the hexagonal phase have been proposed including a liquid crystal templating mechanism,[2] tubular silica encapsulation around the external surface of surfactant micelles followed by spontaneous assembling of these rod-like species into hexagonal packing[2,6] (hereafter, rod mechanism), and a lamellar to hexagonal phase transformation mechanism[5a] (hereafter, layer mechanism).

All the syntheses so far have been carried out under conventional hydrothermal conditions starting from reaction

* Author to whom correspondence should be addressed.

[⊗] Abstract published in *Advance ACS Abstracts*, September 1, 1995.

(1) Kresge, C. T.; Leonowicz, M. E.; Roth, W. J.; Vartuli, J. C.; Beck, J. S. *Nature* **1992**, *359*, 710−712.

(2) Beck, J. S.; Vartuli, J. C.; Roth, W. J.; Leonowicz, M. E.; Kresge, C. T.; Schmitt, K. D.; Chu, C. T.-W.; Olson, D. H.; Sheppard, E. W.; McCullen, S. B.; Higgins, J. B.; Schlenker, J. L. *J. Am. Chem. Soc.* **1992**, *114*, 10834−10843.

(3) Hou, Q.; Margolese, D. I.; Ciesla, U.; Feng, P.; Gier, T. E.; Sieger, P.; Leon, R.; Petroff, P. M.; Schüth, F.; Stucky, G. D. *Nature* **1994**, *368*, 317−321.

(4) Chen, C. Y.; Li, H. X.; Davis, M. E. *Microporous Mater.* **1993**, *2*, 17−26.

(5) (a)Monnier, A.; Schüth, F.; Huo, Q.; Kumar, D.; Margolese, D.; Maxwell, R. S.; Stucky, G. D.; Krishnamurty, M.; Petroff, P.; Firouzi, A.; Janicke, M.; Chmelka, B. F. *Science* **1993**, *261*, 1299−1303. (b) Huo, Q.; Margolese, D. I.; Ciesla, U.; Demuth, D. G.; Feng, P.; Gier, T. E.; Sieger, P.; Firouzi, A.; Chmelka, B. F.; Schüth, F.; Stucky, G. D. *Chem. Mat.* **1994**, *6*, 1176−1191. (c) Stucky, G. D.; Monnier, A.; Schüth, F.; Huo, Q.; Kumar, D.; Margolese, D.; Krishnamurty, M.; Petroff, P.; Firouzi, A.; Janicke, M.; Chmelka, B. F. *Mol. Cryst. Liq. Cryst.* **1994**, *240*, 187−200.

(6) Chen, C. Y.; Burkett, S. L.; Li, H. X.; Davis, M. E. *Microporous Mater.* **1993**, *2*, 27−34.

(7) Vartuli, J. C.; Schmitt, K. D.; Kresge, C. T.; Roth, W. J.; Leonowicz, M. E.; McCullen, S. B.; Hellring, S. D.; Beck, J. S.; Schlenker, J. L.; Olson, D. H.; Sheppard, E. W. *Stud. Surf. Sci. Catal.* **1994**, *84A*, 53−60.

(8) Feuston, B. P.; Higgins, J. B. *J. Phys. Chem.* **1994**, *98*, 4459−4462.

(9) Alfredsson, V.; Keung, M.; Monnier, A.; Stucky, G. D.; Unger, K. K.; Schüth, F. *J. Chem. Soc., Chem. Commun.* **1994**, 921−922.

(10) Schmidt, R.; Akporiaye, D.; Stöcker, M.; Ellestad, O. H. *J. Chem. Soc., Chem. Commun.* **1994**, 1493−1494.

(11) Janicke, M.; Kumar, D.; Stucky, G. D.; Chmelka, B. F. *Stud. Surf. Sci. Catal.* **1994**, *84A*, 243−250.

(12) Schmidt, R.; Akporiaye, D.; Stöcker, M.; Ellestad, O. H. *Stud. Surf. Sci. Catal.* **1994**, *84A*, 61−68.

(13) Bellussi, G.; Perego, G.; Carati, A.; Peratello, S.; Massara, E. P.; Perego, G. *Stud. Surf. Sci. Catal.* **1994**, *84A*, 85−92.

(14) Coustel, N.; Di Renzo, F.; Fajula, F. *J. Chem. Soc., Chem. Commun.* **1994**, 967−968.

(15) Akporiaye, D.; Hansen, E. W.; Schmidt, R.; Stöcker, M. *J. Phys. Chem.* **1994**, *98*, 1926−1928.

(16) Branton, P. J.; Hall, P. G.; Sing, K. S. W. *J. Chem. Soc., Chem. Commun.* **1993**, 1257−1258.

(17) Inagaki, S.; Fukushima, Y.; Kuroda, K. *J. Chem. Soc., Chem. Commun.* **1993**, 680−682.

(18) Wu, C. G.; Bein, T. *Science* **1994**, *264*, 1757−1758.

(19) Wu, C. G.; Bein, T. *Stud. Surf. Sci. Catal.* **1994**, *84C*, 2269−2276.

(20) Behrens, P.; Stucky, G. D. *Angew. Chem., Int. Ed. Engl.* **1993**, *32*, 696−699.

(21) Tanev, P. T.; Chibwe, M.; Pinnavaia, T. J. *Nature* **1994**, *368*, 321−323.

(22) Corma, A.; Navarro, M. T.; Pérez-Pariente, J. *J. Chem. Soc., Chem. Commun.* **1994**, 147−148.

(23) Corma, A.; Navarro, M. T.; Pérez-Pariente, J.; Sánchez, F. *Stud. Surf. Sci. Catal.* **1994**, *84A*, 69−75.

(24) Franke, O.; Rathousky, J.; Schulz-Ekloff, G.; Stárek, J.; Zukal, A. *Stud. Surf. Sci. Catal.* **1994**, *84A*, 77−84.

(25) Reddy, M. K.; Moudrakovski, I.; Sayari, A. *J. Chem. Soc., Chem. Commun.* **1994**, 1059−1060.

(26) Harris, R. K.; Knight, C. T. G. *J. Mol. Struct.* **1982**, *78*, 273−278.

(27) Wiebcke, M.; Grube, M.; Koller, H.; Engelhardt, G.; Felsche, J. *Microporous Mater.* **1993**, *2*, 55−63.

0002-7863/95/1517-9709$09.00/0

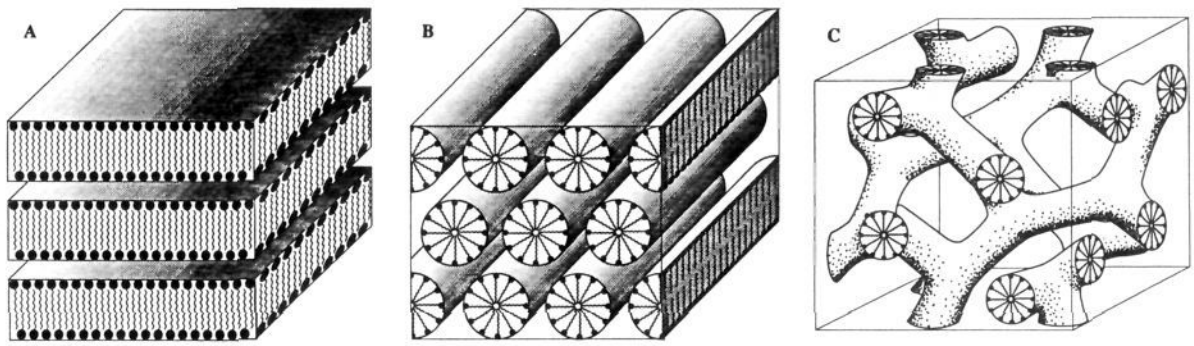

Figure 1. A schematic presentation of three inorganic-surfactant mesostructures: (A) the lamellar phase, (B) the hexagonal phase, and (C) the "bicontinuous" cubic (*Ia3d*) phase. Note that only the surfactant parts of the structures are presented for clarity. In real materials, all the empty spaces in the figures between the surfantant assemblies (rods, layers, etc.) are filled with extended inorganic frameworks. Part C is adapted from ref 31.

mixtures of surfactants and oxide gels produced from either inorganic or alkoxide precursors. Due to the complex nature of gel precursors, which may contain both colloidal particles and hydrolyzed polymeric species each with many different structural and compositional features, it is difficult to follow the evolution of the structure during synthesis and to understand the mechanistic pathways. As pointed out by Stucky and co-workers,[5] the electrostatic interaction and the matching of charge density at the inorganic−surfactant interfaces should govern the cooperative assembly of these mesostructures. Therefore, in order to achieve controlled structure organization and attain more control over the structure tailoring of these materials, one has to manage to control or to adjust the electrostatic interaction and the charge density matching at the interfaces. For this purpose, oxide gels may well not be the most appropriate precursor species. In the present work, we have introduced a degree of ordering into the materials by starting from well-characterized polysilicate species and controlling the degree of condensation by acidic vapor treatment of polysilicate−surfactant mesophasic precipitates.

Experimental Section

The precipitation and structure organization of Si_8 anions with *n*-hexadecyltrimethylammonium chloride ($C_{16}TACl$) was carried out at room temperature (RT) by mixing a solution of $[N(Me)_4]_8Si_8O_{20}{\cdot}65H_2O$ (TMA-Si_8) crystals and a solution of $C_{16}TACl$, to which, if needed, a suitable amount of acid or base was added before mixing. Freshly prepared and relatively concentrated TMA-Si_8 solutions were used to avoid possible condensation of the silicate anions before they were mixed with the surfactant. Typically, a 20-mL solution containing 2 g of TMA-Si_8 crystals and a 100 mL 5% $C_{16}TACl$ solution were used in each precipitation experiment. The acid and base used were $N(Me)_4OH{\cdot}5H_2O$ and concentrated (38%) HCl solution, respectively. The pH values were about 11 for the precipitate mixtures containing base and in the range 1.5−4.5 for those containing acid. The precipitates formed immediately and then were aged in their mother liquor for 3 h at room temperature before being filtered or centrifuged. There was no structural change during this aging period at high pH, but it was necessary at lower pH to achieve a reproducible degree of condensation. TMA-Si_8 crystals were prepared according to a previously reported procedure[28] by first dissolving Ludox silica in a solution of $N(Me)_4OH$ (TMAOH) and then slowly evaporating the solution over concentrated H_2SO_4.

Vapor-phase treatments for structure-ordering or structure-transformation studies of the precipitate phases were performed using a procedure similar to the vapor phase transport technique described in the literature for the synthesis of zeolite molecular sieves.[29] Briefly, our procedure involved the acidic vapor treatments of the precipitates at 105−130 °C using a steel bomb with Teflon linings and a small Teflon cup to separate the solid sample from the liquid phase below it. Details about the reaction vessel are given in ref 29. Typically, 0.3-g solid samples and 10 mL of 0.44% HCl solution were used in each experiment. Treated samples were washed with distilled water and then air-dried before physical measurements were carried out.

Analytical data (sample, % N, % SiO_2, XRD): L_0, 3.13, 14.27, Figure 3a; L_1, 2.18, 38.0, Figure 3c; H_0, 2.83, 30.18, Figure 3d; H_1, 2.47, 48.71, Figure 3e.

X-ray diffraction patterns were obtained on a Rigaku Rotaflex rotating anode diffractometer using Cu Kα radiation. Solid state ^{29}Si and ^{27}Al MAS NMR spectra were obtained with a spinning rate of about 3 KHz on a Bruker AM-400 NMR spectrometer using a homemade MAS probe. The ^{29}Si and ^{27}Al chemical shifts were referenced to TMS using Q_8M_8 as an intermediate reference for ^{29}Si and the $Al(H_2O)_6^{3+}$ resonance of a 1 M solution of aluminium nitrate as external reference for ^{27}Al. The ^{29}Si spectra were obtained without cross polarization, and with long delays and short 30° pulses to ensure quantitative reliability.

Results and Discussion

Our new approach to the synthesis of mesostructural systems is based on the Scheme 1. Instead of using heterogeneous gels, we initiated our syntheses from clear solutions of polysilicate species, specifically, the well-known cube-like double four-ring (D4R) silicate, $Si_8O_{20}^{8-}$ (Si_8), which has been well characterized in both solution and the crystalline solid state, for example as its tetramethylammonium (TMA) salt, $(TMA)_8Si_8O_{20}{\cdot}65H_2O$,[26,27] by NMR and X-ray diffraction techniques. First, the strong electrostatic interactions between the Si_8 anions and the surfactant cations make it possible to easily and cleanly obtain mesophasic precipitates which show different organized structures depending on the charge density (charge to volume ratio) of the inorganic precursors (Step I). Further modification of the structure through condensation can be achieved by acidic vapor treatments of the precipitates resulting in highly ordered mesostructural materials (Step II). Using this procedure, it is possible to synthesize the lamellar, the cubic-*Ia3d*, and the hexagonal mesostructures (Figure 1) in a simpler, more reliable and more understandable manner, and it is also possible, for the first time, to document structural transformations between these mesophases in a systematic way. For clarity of presentation these topics will be discussed separately. It should be noted that since a two-step process is involved in the present work, these are not true phase transitions and the results cannot be compared directly to data from "in situ" solution preparations. For this reason, we refer to them as structural transformations.

Figure 2 presents the XRD patterns and ^{29}Si MAS NMR spectra of the $Si_8C_{16}TA$ precipitates obtained through the above

(28) Fyfe, C. A.; Fu, G.; Grondey, H. *Better Ceramics Through Chemistry VI*, in press.

(29) Kim, M. H.; Li, H. X.; Davis, M. E. *Microporous Mater.* **1993**, *1*, 191−200.

Scheme 1

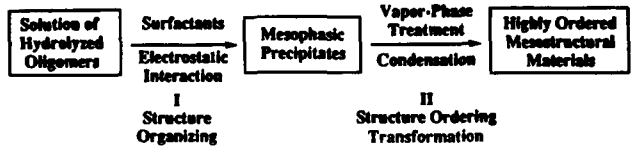

procedure with $C_{16}TACl$ reagent solutions in which different amounts of tetramethylammonium hydroxide (TMAOH) or hydrochloric acid (HCl), as described in the figure caption, were added before the solutions were combined and precipitation occurred. The reaction conditions were otherwise identical. From a comparative examination of these XRD patterns, it is clear that they are due to two different mesophases. One forms in basic or neutral surfactant solutions (Figure 2, a and b) and clearly shows a layer-based structure. Its ^{29}Si NMR spectrum has a single, narrow peak at −99 ppm, which is virtually the same as that of the Si_8 anions in their crystalline TMA salt,[28] indicating the Si_8 structural units are perfectly intact in this layered mesophase. We denote this phase as L_0. When acid is added to the surfactant solutions, another mesophase appears (Figure 2, c and d) and the ^{29}Si NMR spectrum shows the expected Q^3 resonance at −99 ppm, and an additional peak at about −110 ppm in the Q^4 Si region indicating that condensation between Si_8 cubes has taken place. When a relatively large amount of acid is used, the second phase is virtually the only one observable in the precipitates (Figure 2, e and f). The XRD pattern of this phase is very close to that of MCM-41 but with less well defined higher order peaks. It is possible that there has been some decomposition of the Si_8 cubes during the condensation process. However, there is no evidence in the ^{29}Si MAS spectrum for any Q^2 sites which would be expected for linear or monocyclic oligomers. Calcination of this phase produced a mesoporous material which had a XRD pattern similar to that of calcined MCM-41 but, again, with poorly defined higher order peaks. In addition, this phase directly transformed into highly ordered hexagonal structure (MCM-41) after treatment with acidic vapor (see below). Therefore, we believe that this precipitate phase is formed by silicate−surfactant mesoscopic rods with poorly ordered hexagonal packing. We denote this phase as H_0. It should be noted that the degree of silicate condensation as indicated by the ^{29}Si NMR spectra in this phase can vary considerably depending on precipitation conditions (Figure 2, e and f). By the terminology "H_0 phase" we refer here to all those rod-based mesophases which are close to but not as well ordered as hexagonal MCM-41.

To try to prove the integrity of the Si_8 system in these phases, we have investigated the FT IR spectra of the precipitates. In the case of zeolites, Flanigen and co-workers have shown that IR spectroscopy is a sensitive tool for the investigation of structural features of the frameworks.[30] Of particular interest, they identified signals occurring in the region 500−650 cm^{-1} as being characteristic of double ring systems, the open frameworks of these systems making it possible to observe the vibrational modes of these distinct structural units. In the present work, the IR spectra of Si_8, completely siliceous zeolite A, and Q_8M_8 chosen as reference compounds show strong absorptions in this range (610 and 555 cm^{-1}) considered due to the D4R moities. By contrast, the $C_{16}TABr$ template shows no absorption in this region. The layered precipitate (L_0) phase precipitated at high pH shows a strong

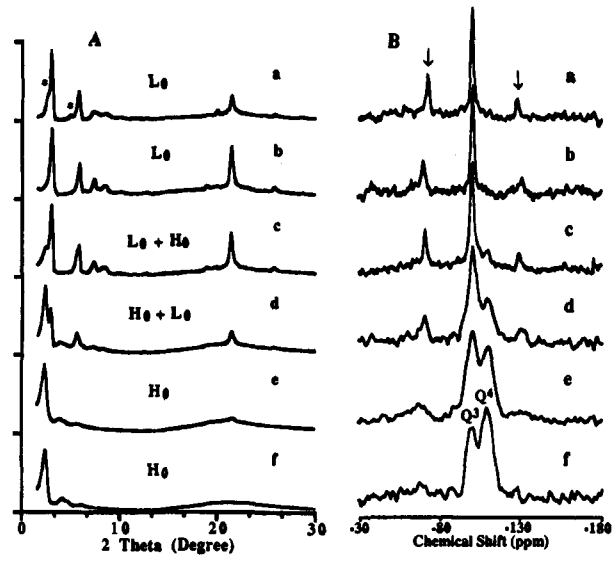

Figure 2. (A) XRD patterns and (B) solid state ^{29}Si MAS NMR spectra of $Si_8C_{16}TA$ precipitates prepared at room temperature by addition of solutions of $(NMe_4)_8Si_8O_{20}{\cdot}65H_2O$ crystals (typically, 2 g in 20 mL of H_2O) into $C_{16}TACl$ solutions (typically, 100 mL of 5 wt %) which contain (a) 5 g of $TMAOH{\cdot}5H_2O$, (b) no additional reagents, and (c−f) 0.1, 0.2, 0.4, and 0.6 mL of 38% HCl solution, respectively. The XRD peaks indicated "*" in (a) are due to another layered mesophase. The NMR peaks indicated "↓" are spinning sidebands.

absorption at 593 cm^{-1} suggesting the presence of a high concentration of D4R in agreement with the ^{29}Si spectra of Figure 2B. This absorption persists in the vapor-treated L_1 phase (see on). The hexagonal precipitate (H_0) obtained at lower pH also shows an absorption at 574 cm^{-1} as does the vapor-treated (H_1) material (see on) indicating the presence of a substantial concentration of D4R units. In contrast, amorphous silica gel shows no clear absorption in the region. The calcined (H_1) hexagonal phase also shows an absorption at 585 cm^{-1}. The corresponding hexagonal phases formed from Al_4Si_4 cubes (see on) which are the stable species at the pH values of their formation also show strong absorptions at (584−590) cm^{-1} again confirming the presence of intact D4R cubes. Although these observations are only semiquantitative in nature, they indicate a considerable degree of stability of the D4R units in these materials and during reactions such as those described in the present work.

Through the vapor-phase treatment, a cubic-*Ia3d* phase (V_1) and a lamellar phase (L_1) have been produced from the precipitate L_0 and a hexagonal phase (H_1) from the precipitate H_0. Figure 3 shows the XRD patterns and ^{29}Si NMR spectra of these highly ordered mesostructures as well as those of the precursor L_0 and H_0 phases for comparison. The shorthand notations used here for these mesophases are mainly based on the nomenclature used by Tiddy for the corresponding surfactant liquid crystal (SLC) phases[31] with some modifications for the lamellar phases. The capital letters designate different mesostructures, L for lamellar, V for cubic-*Ia3d*, etc., and the subscript 1 designates, in the case of lamellar phases, a structure with surfactant monolayers between the silicate framework layers and, in the other cases, a normal structure in which the silicate part is continuous throughout the structure. We use subscript 0 to designate the precipitate phases.

The XRD patterns of the V_1, L_1, and H_1 phases shown in Figure 2 exactly match those reported in the literature for the corresponding mesostructures. The bicontinuous cubic structure V_1 has been extensively studied for SLC phases[31,32] and recently

(30) (a) Flanigen, E. M. In *Zeolite Chemistry and Catalysis*; Rabo, J. A., Ed.; ACS Monograph No. 171; American Chemical Society: Washington, DC, 1976; p 80. (b) Flanigen, E. M.; Khatami, H.; Szymanski, H. A. *Adv. Chem. Ser.* **1971**, *101*, 201.

(31) Tiddy, G. J. T. *Phys. Rep.* **1980**, *57*, 1−46.

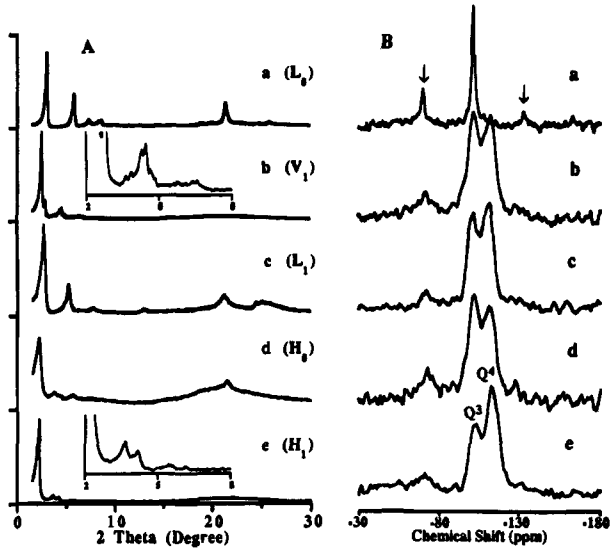

Figure 3. (A) XRD patterns and (B) solid state ^{29}Si MAS NMR spectra of the $Si_8C_{16}TA$ mesophases: (a) layered L_0 phase obtained by direct precipitation (see Figure 1 for details), (b) the cubic V_1 (*Ia3d*) produced by acidic vapor treatment of L_0 at 110 °C for 7 days, (c) the lamellar L_1 phase from treating L_0 at 128 °C for 8 days, (d) the rod-based precipitate H_0 prepared by precipitation under acidic conditions (see Figure 1), and (e) the hexagonal H_1 phase obtained from H_0 by acidic vapor treatment at 110 °C for 7 days. The insets in patterns b and e show the higher order XRD peaks enlarged. The NMR peaks indicated "↓" are spinning sidebands.

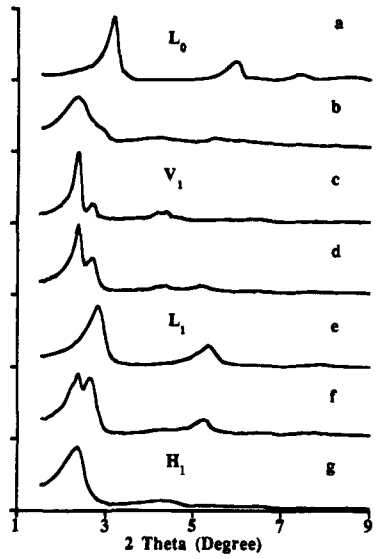

Figure 4. XRD patterns showing the structural transformations of the L_0 precipitate phase during an acidic vapor treatment. (a) The layered L_0 used for experiments (b–g) under the following conditions: (b–d) treatment with 0.44% HCl solution, 110 °C, and 1, 5, and 10 days, respectively; (e–g) treatment with 0.44% HCl solution, 130 °C and 8, 12, and 24 days, respectively. (c), (e), and (g) are typical patterns of the V_1, L_1, and H_1 mesophases, respectively.

discovered as one of the inorganic–surfactant mesostructures (ISM).[2,5,7] Such a structure may be viewed as two intertwined and unconnected 3-D networks of self-assembled short surfactant rods, joined coplanarly 3 by 3, with a single, infinite silicate network filling the spaces between the surfactant rods.[32] The L_1 phase obtained here clearly shows a more highly ordered structure than those reported for a similar lamellar phase as indicated by the better defined high-order X-ray reflections which are even observable in the region of 20–30° 2θ.[2,7] The ^{29}Si NMR spectrum (Figure 3) shows that in L_1 more than 50% of the Si atoms are in Q^4 sites indicating condensed silicate layers. In fact, the XRD pattern of L_1 is very similar to those of $C_{16}TA^+$ pillared layered silicates such as Kanemite and Magadiite.[33] In this sense, L_1 is quite different from L_0 where the silicate layers are formed by individual Si_8 anions although both phases show comparable interlayer distances ($d_{100} \approx 32$ Å for L_1 and $d_{100} \approx 29$ Å for L_0) and both consist of surfactant monolayers. At this point, both L_1 and L_0 are different from the bilayer phase (L_α) commonly observed in SLC systems.[31]

Previously, syntheses of the mesostructural materials reported in the literature commonly involved complex recipes and procedures until recently Vartuli et al.[7] reported a simple system consisting of only TEOS (tetraethylorthosilicate) and $C_{16}TA$ hydroxide solution for the synthesis of silica mesostructures. The two-step synthesis procedure we have used here (Scheme 1) may be preferable to the existing literature methods because it not only involves a simple recipe and procedure but also makes the reaction parameters controllable and adjustable. In addition, it provides one possible way to tailor-make these mesostructures in terms of both composition and structure.

One of the most important advantages of the vapor phase procedure is that it allows the direct observation of the structural transformations between these mesostructures. Figure 4 shows the XRD patterns of a series of L_0 samples (pattern **a**) treated with acidic vapor as a function of time under the conditions given in the figure caption. It can be seen that the patterns **c**, **e**, and **g** in the figure are due to the cubic (V_1), the lamellar (L_1), and the hexagonal (H_1) structures, respectively although the H_1 structure here does not show well-defined high-order peaks. Calcination experiments confirm that this phase is indeed the hexagonal structure rather than another lamellar phase and that it is thermally stable. The patterns **b**, **d**, and **f** in the figure are given to show the intermediate structure (**b**) or mixtures of structures (**d** and **f**) observed when the structures are transformed from one to another. Therefore, these mesophases transform in the following order

$$L_0 \rightarrow V_1 \rightarrow L_1 \rightarrow H_1$$

It is possible to understand these transformation processes by comparison with the corresponding changes observed for the SLC systems, where the following typical phase transformation scheme as a function of surfactant concentration has been well established in the order of decreasing concentration:[31]

$$\text{lamellar } (L_\alpha) \leftrightarrow \text{cubic } (V_1) \leftrightarrow \text{hexagonal } (H_1) \leftrightarrow \text{cubic } (I_1) \leftrightarrow \text{micelles}$$

It is well-understood that the addition of water (dilution) to a concentrated system with an L_α SLC phase decreases the charge density of the inorganic (water) region and correspondingly increases the volume ratio of the surfactant polar heads to apolar chains, therefore increasing the curvature of the water–surfactant interfaces. As a result, one sees the transformation from flat bilayer L_α (0 curvature), to the "saddle-splay" curvature V_1, to circular cylinders H_1, to sphere-based I_1, and finally to spherical micelles (maximum curvature).[31] We believe that very similar processes govern the pathway of the structural transformations of our Si_8-$C_{16}TA$ systems. During the acidic vapor treatment, protons neutralize the negative charges of the silicate anions, and therefore decrease the charge density of the inorganic (silicate) region and increase the head-to-chain volume

(32) (a) Seddon, J. M.; Templer, R. H. *Phil. Trans. R. Soc. London A* **1993**, *344*, 377–401. (b) Mariani, P.; Luzzati, V.; Delacroix, H. *J. Mol. Biol.* **1988**, *204*, 165–189.

(33) Schwieger, W.; Fyfe, C. A. Unpublished results.

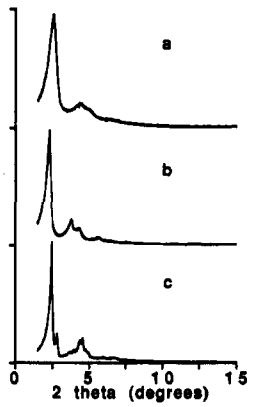

Figure 5. XRD patterns of the silicate mesostructures calcined by slowly increasing the temperature to 550 °C in N_2 atmosphere and then heating at 550 °C for 5 h in air: (a) precipitate H_0 phase; (b) hexagonal H_1 phase obtained from H_0 by acidic vapor treatment; and (c) cubic V_1 phase obtained from the L_0 phase by acidic vapor treatment.

ratio of the surfactant assembly. As a result, the transformations which occur are from one structure with a lower head-to-chain volume ratio to another with a higher ratio. In general, these silicate mesostructures are stable to calcination and template removal. Figure 5 shows the XRD patterns of the precipitate H_0, hexagonal H_1, and cubic V_1 structures. Comparison of the patterns with those of the uncalcined forms shown in Figures 2e, 2f, and 3b, respectively, shows that the structures are unchanged, and the ordering may even improve somewhat as in the case of the H_1 phase.

There is an important difference between the transformation processes of the ISM phases and the SLC phases. For the SLC phases, the charge density change is achieved simply from the change of the water volume and the number and identities of the charged species (e.g., Cl^- in the $C_{16}TACl$ system) remain the same during the phase transformation. For the ISM phases, on the other hand, the charge density decrease is accompanied by chemical processes such as protonation and, especially, condensation, while the total volume of the silicate part is not substantially changed. As a result, some surfactant cations have to be removed from the structure to maintain charge balance. Obviously, it is the condensation process that produces an extended silicate framework which can be stable even after the subsequent removal of all the surfactants. Since condensation is involved, the flexibility of a partially condensed framework to adapt to the geometry required by a mesophase is an important factor in facilitating the transformation.

It is somewhat surprising that a lamellar phase L_1 appears between the cubic V_1 and the hexagonal H_1 phases as this is not observed for the SLC systems. As shown by the ^{29}Si NMR data in Figure 3, the degree of condensation is slightly higher for L_1 than for V_1, which means that the charge density of the silicate part is lower for L_1. However, a lamellar structure should require a higher charge density at the interfaces than a cubic one with curved interfaces. We believe that the transformation from V_1 to L_1 is accompanied by an increase in the silicate wall thickness so that, even though the charge density for the whole silicate framework decreases, it increases at the interfaces. The increase of the basal spacings from L_0 to L_1 as indicated by the reflections in Figure 3 indicates an increase in wall thickness although it is hard to estimate the exact wall thickness of the V_1 structure. Nevertheless, since in V_1 the interface curvature varies continuously throughout the structure and a positive curvature in one direction is balanced by a negative one at right angles to it, the average curvature is not very different from that of a lamellar phase.[31]

Scheme 2

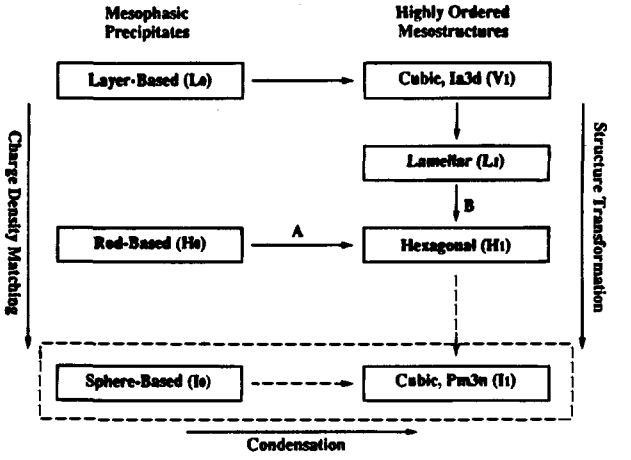

Scheme 2 summarizes the results discussed above together with two additional reaction pathways which we predict may be possible for similar materials based on these results (indicated by the box in dashed lines). As can be seen in the scheme, both the "rod mechanism" (labeled A) and the "layer mechanism" (labeled B) mentioned above are possible, but neither one completely describes the mechanistic pathways found for these phases. It is clear that the silicate–surfactant mutual organization governed by electrostatic interactions is a determining factor in the formation of the mesophases.[5] We believe that this mutual organization process first leads to silicate–surfactant assemblies with simple geometries, discs, rods, or spheres, depending on the charge density or the degree of condensation of the silicates involved, and these assemblies then further condense into extended structures. In the latter process, the identities or geometries of the silicate–surfactant assemblies may be either maintained or transformed depending on the final reaction parameters (pH, temperature, etc.). This mechanism is supported by our results as discussed above, particularly by the fact that we have obtained the Si_8-$C_{16}TA$ mesophasic precipitates (L_0 and H_0) with layer and rod-based geometries by simply mixing two solutions together. Silicate–surfactant assemblies with more complicated geometries are unlikely to exist at the very initial stages of structure growth. This is probably why, as we observed in the precipitation experiments, the disordered analogue of the complicated V_1 phase could not be obtained by direct precipitation although its degree of condensation should be between that of L_0 and H_0 (Figures 2 and 3).

When the silicate species involved are relatively small and highly charged as is probably the case at the early stage of a hydrothermal synthesis at high pH and for the precipitates we obtained under basic conditions, there are no essential differences between the general structural characteristics of silicate–surfactant systems and those of the surfactants themselves with simple counterions. It is the fact that the Krafft temperature[34] is above room temperature for the Si_8-$C_{16}TA$ system that makes it possible for us to isolate the mesophasic precipitates. We have observed that at elevated temperatures (~50 °C) the precipitates redissolve. Assuming that the Si_8-$C_{16}TA$ system can be controlled so that further condensation of the Si_8 polyanions can be effectively prevented at the temperature above the Krafft boundary, what we predict is most likely a Si_8-C_{16}-TA micelle solution at low concentration and lyotropic liquid crystal phases when the concentration is higher. Under normal

(34) The Krafft temperature is a characteristic temperature for surfactant–water systems at a specific concentration of surfactant, below which the surfactant precipitates from solution.

conditions for the synthesis of mesostructures,[2-4] such lyotropic liquid crystal phases are unlikely to exist because not only is the concentration normally much lower than required for these phases but also the progressive condensation of the silicates would make the silicate–surfactant assemblies lose their lyotropic character. However, they may still behave similarly to thermotropic liquid crystals. It has been known that anhydrous surfactants form liquid crystal phases in the temperature ranges between those of the crystalline solid and the amorphous liquid (melt).[31] The formation of these thermotropic phases is the result of a balance of the strong electrostatic interaction between counterions and head groups and the week attractive forces between alkyl chains. The former causes a tendency to form regular crystals but the latter is a driving force toward the liquid state. We have observed that vapor phase treatment of the precipitated L_0 phase at around 110 °C changes it to a transparent material similar to the "waxy" (liquid crystal) phases reported in surfactant systems.[31] When cooled to room temperature it remains transparent and still shows a high degree of order. Based on these observations, the formation of the mesophases may be understood as operating by a liquid crystal mechanism. The strong similarities between ISM materials and SLC phases in terms of structure and behavior clearly indicate that these two systems must be closely related. The tendency for the silicate–surfactant systems to form mesophases resembling liquid crystals is most likely resposible for the disordered framework in the ISM materials.

Using the two-step synthetic procedure described above, we have also prepared a hexagonal aluminosilicate mesostructure (AS-H_1) with a Si/Al ratio close to 1 from the known aluminosilicate analogue of Si_8, the $Al_4Si_4(OH)_8O_{12}^{4-}$ (Al_4Si_4) species. A detailed description of this new aluminosilicate material will be given elsewhere. Here we wish only to mention one interesting aspect of the behavior of the Al_4Si_4 anions observed in our precipitation experiments. For Al_4Si_4, when mixed with $C_{16}TA$, the rod-based precipitate phase (AS-H_0) is always the dominant product even under basic conditions (pH $\approx$ 10). Under these conditions, however, only the layered precipitate phase (L_0) is formed for Si_8 (see above). This is understandable because Al_4Si_4 (4−) has a lower charge than Si_8 (8−), and since all the terminal groups in the Al_4Si_4 structure are OH (but O^- in Si_8), condensation can take place much more easily even under basic conditions, which further lowers the charge density. Obviously, such a precursor is unfavorable for an L_0 phase which requires highly charged inorganic layers. This observation provides additional evidence that the charge density of the inorganic precursor is one of the important factors that determine the structure of the mesophase formed from it.

In summary, the synthesis of ISM materials using a two-step procedure from oligomeric precursors such as cubic Si_8 and Al_4Si_4 has been clearly demonstrated. In the structure organization step, either layer-based or rod-based mesophasic precipitates can be obtained by controlling the charge density of the silicate precursors. A sphere-based precipitate phase is also predicted although it has not been obtained in this work (Scheme 2). In the structure ordering and transformation step, the vapor phase technique has allowed us to obtain all the reported highly ordered mesophases (except the I_1 structure) and to observe the structural transformations step by step between these phases. Valuable information about the mechanistic pathways leading to the formation of these mesophases has also been derived from these results. As demonstrated by the data on Al_4Si_4, incorporation of high concentrations of Al which is very difficult with other methods[10-12] can be better achieved in the oligomer stage. Obviously, other metallic elements could also be incorporated into these silicate mesostructures in a similar fashion.

The synthetic procedure may also be extended to other inorganic oligomer–surfactant systems. Considering the great diversity in terms of structure and composition of both inorganic oligomers (e.g., polyanions and polycations) and surfactants, the possibilities are endless. The size and charge of an oligomeric species are among the most important parameters that need to be considered when one designs a mesostructure although the ability of the precursor species to condense into an extended framework is also crucial if a thermally stable mesoporous framework is to be formed. The modification of the charge densities of the oligomeric precursors, as we have done in this work, is a very convenient way to control the charge density matching at the interfaces to achieve a desired mesostructure but it is certainly not the only way. It could also be achieved by a modification of the surfactant component. For example, partial replacement of $C_{16}TA$ with similar but shorter chain surfactants would reduce the chain volume and make formation of a mesostructure with curved interfaces more favorable regardless of whether the oligomers are highly charged. A similar effect is also predicted for multiple-charged surfactants. On the other hand, double chain surfactants or mixtures of charged and neutral surfactants with the same chain lengths would favor structures with low curvatures such as lamellar phases. It should also be mentioned that, if only typical M41S materials are desired, the two-step synthesis procedure reported here may be replaced by a single-step synthesis in solution from the same precursors if the appropriate conditions are chosen. Similarly, the well-characterized TMA-Si_8 precursor solution used here may be replaced by a NaOH-hydrolyzed solution which typically contains a broad spectrum of soluble silicate species.[37] However, we believe that a more easily controllable procedure and the use of well-characterized oligomeric precursors, possibly utilizable as building blocks, could be advantageous as far as structure tailoring and framework ordering of the final materials are concerned.

Acknowledgment. We thank Dr. W. Schwieger, Dr. G. T. Kokotailo, Dr. H. Grondey, and Dr. Yiu Lau Lam for many helpful discussions and Dr. Yining Huang for his help and advice on the IR experiments. G.F. gratefully acknowledges the NSERC of Canada for financial support in the form of a Postdoctoral Fellowship. C.A.F. acknowledges the financial support of the NSERC of Canada in the form of Operating and Equipment Grants.

JA9433075

(35) Engelhardt, G.; Hoebbel, D.; Tarmak, M.; Samoson, A.; Lippmaa, E. *Z. Anorg. Allg. Chem.* **1982**, *484*, 22–32.

(36) Grube, M.; Wiebcke, M.; Felsche, J.; Engelhardt, G. *Z. Anorg. Allg. Chem.* **1993**, *619*, 1098–1104.

(37) Engelhardt, G.; Rademacher, O. *J. Mol. Liq.* **1984**, *27*, 125–131.